# Supporting Information

## Han et al. 10.1073/pnas.1106386108

### SI Methods

**Plasmid Construction.** ***CD8-GFP variants in pAPIC.*** The *ppk* enhancer, the CD8-GFP coding sequence, the synthetic intron, and all core promoter-5′UTR and 3′UTR-polyA fragments were amplified by PCR (Table S1). A fragment (referred to as PH) containing *ppk* enhancer (between NotI and and NheI) and *hsp70* core promoter-5′UTR (between NheI and XhoI), and a fragment (referred to as CH) containing the CD8-GFP coding sequence (between XhoI and PacI) and *His2Av* 3′UTR-polyA (between PacI and SpeI), were independently assembled in pPelican-H Green (1) by three-way ligation. A SalI fragment containing an attB site was isolated from pAttB (2) and inserted into the NdeI site of pGreen H-Pelican by blunt ligation. The resulted vector was then used to assemble PH-CH through three-way ligation between NotI and SpeI to make pAPIC-PHCH. The *His2Av* fragment of pAPIC-PHCH was replaced by the 3′UTR-polyA fragments from SV40 early genes and *α-Tub1* to make pAPIC-PHCS and pAPIC-PHCT, respectively. The PH fragment of pAPIC-PHCH was replaced by *ppk* enhancer and its endogenous core promoter-3′UTR to make pAPIC-PCH, and was replaced by *ppk* enhancer-core promoter-3′UTR and the synthetic intron through three-way ligation to make pAPIC-PsICH. The synthetic intron was inserted after the *hsp70* fragment of pAPIC-PHCH to make pAPIC-PHsICH. The *hsp70* fragment of pAPIC-PHCH was replaced by another *hsp70* fragment containing the *z* second intron at the 3′ end to make pAPIC-PHzICH. The *hsp70* fragment of pAPIC-PHCH was replaced by a fragment generated by overlap extension PCR containing *eve* core promoter-3′UTR and the synthetic intron to make pAPIC-PEsICH. The *His2Av* fragment of pAPIC-PHzICH was replaced by the 3′UTR-polyA fragments from SV40 early genes to make pAPIC-PHzICS.

***CD4-GFP, CD4-tdGFP, and CD4-tdTom in pAPIC.*** The CD8 fragment in pAPIC-PHzICH was replaced by a fragment (referred to as CD4) generated by overlap extension PCR containing a synthetic signal peptide (sSP) and CD4 transmembrane domain to make pAPIC-ppk-CD4-GFP. The *ppk* enhancer in pAPIC-ppk-CD4-GFP was then removed and religated by blunt ligation to make pAPIC-sSP-CD4-GFP. A tdGFP fragment was assembled with a copy of EGFP and a copy of GFP by three-way ligation to replace the GFP in pAPIC-sSP-CD4-GFP. The resulted vector pAPIC-sSP-CD4-tdGFP was then used as the template for amplifying another version of tdGFP containing endoplasmic reticulum (ER) exit signals from Kir2.1. The tdGFP in pAPIC-sSP-CD4-tdGFP was replaced by tdGFP-ERs to make pAPIC-sSP-CD4-tdGFP- $ER^{Kir2.1}$. The sSP in pAPIC-sSP-CD4-tdGFP-$ER^{Kir2.1}$ was replaced by annealed oligos encoding signal peptides from *Drosophila Akh*. pAPIC-Akh-CD4-tdGFP-$ER^{Kir2.1}$ was abbreviated as pAPIC-CD4-tdGFP. A tdTom fragment containing the ER exit signal from Kir2.1 was amplified by PCR and use to replace tdGFP-$ER^{Kir2.1}$ in pAPIC-CD4-tdGFP to make pAPIC-CD4-tdTom.

***pDEST-HemmarG/R and ppk-CD4-tdGFP and ppk-CD4-tdTom in pAPIC.*** The RfA cassette was inserted into the BglII site of pAPIC-CD4-tdGFP and pAPIC-CD4-tdTom by blunt ligation to make destination vectors pDEST-HemmarG and pDEST-HemmarR, respectively (Hemmar: destination vectors with high expression membrane marker, green or red). The *ppk* enhancer was cloned into pDONR221 by BP reaction to make pENTR-ppk. LR reactions were then carried out between pENTR-ppk and the Hemmar destination vectors to make pHemmarG-ppk (or pAPIC-ppk-CD4-tdGFP) and pHemmarR-ppk (or pAPIC-ppk-CD4-tdTom).

***CNS-CD4-tdTom in the HemmarR vector.*** Selected neuronal enhancers in Gateway entry vectors were cloned into pDEST-HemmarR by LR reactions.

***pACU2, a high expression upstream activator sequence (UAS) vector, UAS-CD4-tdGFP variants, and UAS-CD4-tdTom.*** The attB fragment isolated from pAttB by SalI digestion was inserted into the NdeI site of pUAST by blunt ligation. The resulted vector was digested by BamHI and used to ligate a BamHI-XbaI fragment from pUAST containing 5× UAS and *hsp70* TATA, and a XbaI-BamHI fragment containing *His2Av* 3′UTR and polyA, through three-way ligation, to make pACU-His. A fragment of synthetic intron with a 5′ MfeI site and a 3′ EcoRI site was amplified by PCR and cloned into the EcoRI site of pACU-His to make pACU2. All six versions of CD4-tdGFP and the CD4-tdTom was isolated from corresponding pAPIC vectors and cloned into pACU2 between the EcoRI and XbaI sites.

**Fly Strains.** The fly strains used in this study are: *ppk-EGFP* (3), *ppk-Gal4* (3), $attP^{VK19}$, $attP^{VK37}$, $attP^{VK33}$ (4), *attP2* (Bloomington), *UAS-CD8-GFP* (Bloomington), *DDC-Gal4* (5), *Tdc2-Gal4* (5), *ort-Gal4* (6), *repo-Gal4* (Bloomington), *A101-Gal4* (Bloomington), *ptc-Gal4* (Bloomington), *UAS-shi$^{ts}$* (7), UAS-EcR-DNF645A, UAS-EcR-DNW650A (Bloomington), and *UAS-Brp-GFP* (8).

***Drosophila* Trangenic Lines.** The integration of attB-containing transgenic vectors into attP docker sites was performed as previously described (9). The *ppk-CD8-GFP* variants in pAPIC vectors were integrated in $attP^{VK19}$; *ppk-CD4-GFP*, *ppk-CD4-tdGFP*, and *ppk-CD4-tdTom* were integrated in *VK19*; *CNS-CD4-tdTom* in the HemmarR vector were integrated in $attP^{VK37}$ or *attP2*; *UAS-CD4-tdGFP* and *UAS-CD4-tdTom* in pACU2 were integrated in $attP^{VK33}$. P-mediated immobilization of *ppk-CD4-tdGFP* and *ppk-CD4-tdTom* was performed according to standard protocols.

**Live Imaging.** For imaging of embryonic ddaC, the embryos was collected on grape agar plates at 25 °C and allowed to develop at 25 °C to appropriate stages, when embryos were dechorionated manually and mounted in halocarbon oil on a glass slide and imaged. For live imaging of larvae and pupae, the animals were reared at 25 °C in density-controlled vials. Third instar larvae at 96 h after egg laying (AEL) were mounted in halocarbon oil and confocal images of ddaC dendrites were collected with a Leica SP5 laser scanning microscope. For live imaging of sensory organ progenitor (SOP) cells in the dorsal thorax, pupae at 20 h after puparium formation (APF) were dissected out from pupal cases and mounted in halocarbon oil for imaging. For live imaging of cytonemes in the wing disk, wing imaginal disks of wandering third instar larvae were dissected out and mounted in PBS on slides. Two layers of double-sided tapes were used as spacers on the slides to prevent flattening of the disks. For time-lapse imaging of dendrite pruning in pupae, white pupae were mounted in an imaging chamber constructed with a thin aluminum slide that has a hole in the middle. The bottom of the hole was covered with an oxygen-permeable membrane (model 5793; YSI) on which pupae was fixed in position with a piece of double-sided tape. The pupae were overlaid with a small amount of halocarbon oil and covered with a coverslip. The time-lapse imaging was carried out at room temperature on a Leica SP5. For experiments involving *UAS-shi$^{ts}$*, control animals and Shi$^{ts}$-expressing animals were reared at room temperature. The pupae were mounted in imaging chambers and shifted to 29 °C in oxygen-

filled, moisturized containers from 3 to 10 h APF. The animals were imaged at room temperature immediately after incubation at 29 °C. The *z*-stack image series were analyzed and projections were produced in the Imaris software (Bitplane AG).

**Quantitative Analysis of Membrane Marker Expression in ddaC.** Single-scan 16-bit images of proximal and terminal dendrites of ddaC neurons in the A2 segment were taken with a 40× NA1.25 oil lens at zoom 6. At least 20 images of proximal and terminal dendrites were taken for each genotypes from at least six animals. Regions of interest (ROIs) were drawn in ImageJ on dendrites and in empty areas for background signals. The pixel intensity of each ROI was measured and averaged and input into MS Excel (Microsoft). The difference between the dendrite signal and the background signal was considered as the net signal. The means and SDs were calculated based on the net signals of all ROIs for each genotype and plotted in charts in Excel.

**Immunocytochemistry.** Staining of larval and adult brains are performed as previously described (10). The primary antibodies used in this study are mouse anti-GFP JL-8 at 1:200 (Clontech), rabbit anti-DsRed at 1:400 (Clontech), and mouse mAb NC82 at 1:100 (Developmental Studies Hybridoma Bank). The primary antibodies were detected by fluorescent-conjugated secondary antibodies from Jackson ImmunoResearch Laboratories. For comparison of neuronal labeling by CD4-tdGFP and CD8-GFP, the samples were imaged directly after fixation without immunostaining.


1. Barolo S, Carver LA, Posakony JW (2000) GFP and beta-galactosidase transformation vectors for promoter/enhancer analysis in *Drosophila*. *Biotechniques* 29:726, 728, 730, 732.
2. Bischof J, Maeda RK, Hediger M, Karch F, Basler K (2007) An optimized transgenesis system for *Drosophila* using germ-line-specific phiC31 integrases. *Proc Natl Acad Sci USA* 104:3312–3317.
3. Grueber WB, Ye B, Moore AW, Jan LY, Jan YN (2003) Dendrites of distinct classes of *Drosophila* sensory neurons show different capacities for homotypic repulsion. *Curr Biol* 13:618–626.
4. Venken KJ, He Y, Hoskins RA, Bellen HJ (2006) P[acman]: A BAC transgenic platform for targeted insertion of large DNA fragments in *D. melanogaster*. *Science* 314: 1747–1751.
5. Vomel M, Wegener C (2008) Neuroarchitecture of aminergic systems in the larval ventral ganglion of *Drosophila melanogaster*. *PLoS One* 3:e1848.
6. Gao S, et al. (2008) The neural substrate of spectral preference in *Drosophila*. *Neuron* 60:328–342.
7. Kitamoto T (2001) Conditional modification of behavior in *Drosophila* by targeted expression of a temperature-sensitive shibire allele in defined neurons. *J Neurobiol* 47(2):81–92.
8. Wagh DA, et al. (2006) Bruchpilot, a protein with homology to ELKS/CAST, is required for structural integrity and function of synaptic active zones in *Drosophila*. *Neuron* 49: 833–844.
9. Venken KJ, et al. (2009) Versatile P[acman] BAC libraries for transgenesis studies in *Drosophila melanogaster*. *Nat Methods* 6:431–434.
10. Wu JS, Luo L (2006) A protocol for dissecting *Drosophila melanogaster* brains for live imaging or immunostaining. *Nat Protoc* 1:2110–2115.


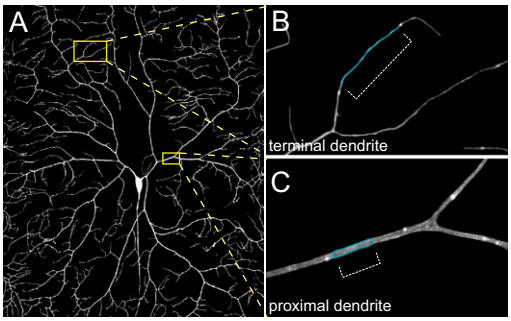


**Fig. S1.** The dendritic tree of the class IV da (C4da) neuron ddaC. (*A*) A class IV dendritic arborization (da) neuron ddaC at 96 h AEL. The larva was oriented anterior left, dorsal up. (*B* and *C*) Magnified views of the boxed regions (*A*) showing ROIs at terminal dendrites (*B*, the blue line) and proximal dendrites (*C*, the area circled by the blue line) for measuring the fluorescent intensities of reporters.

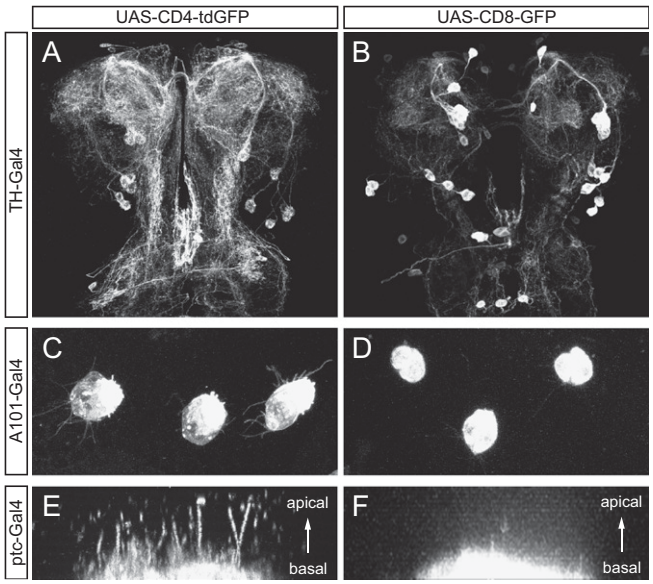


**Fig. S2.** Comparison of CD4-tdGFP and CD8-GFP. (*A* and *B*) Labeling of neurites by *UAS-CD4-tdGFP* (*A*) and *UAS-CD8-GFP* (*B*) driven by *TH-Gal4* in third instar larval brains. (*C* and *D*) Labeling of sensory organ progenitor cells by one copy of *UAS-CD4-tdGFP* (*C*) and two copies of *UAS-CD8-GFP* (*D*) driven by *TH-Gal4* in pupal notums. (*E* and *F*) Labeling of apical membrane extensions of wing disk epithelial cells by one copy of *UAS-CD4-tdGFP* (*E*) and two copies of *UAS-CD8-GFP* (*F*) driven by *ptc-Gal4*.

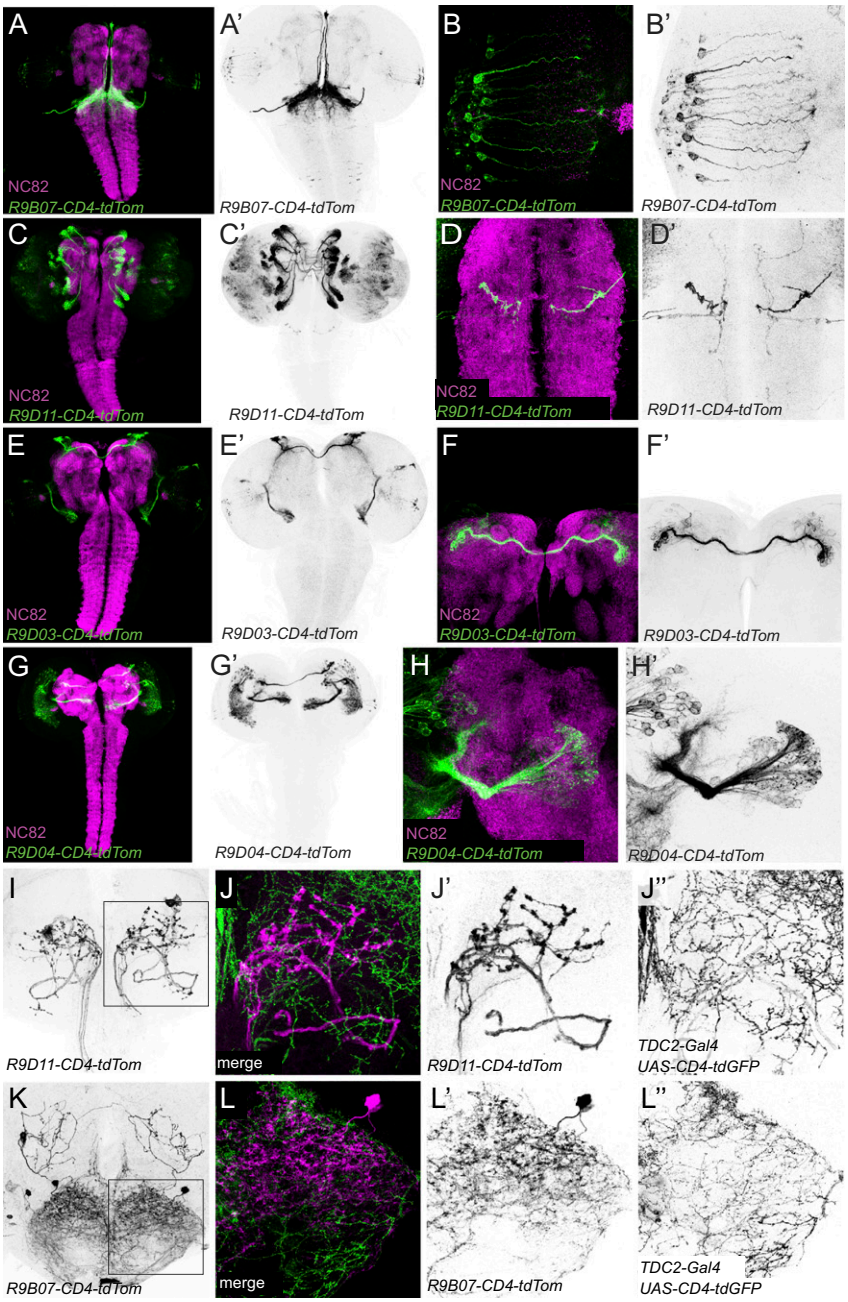


**Fig. S3.** Neuronal projections visualized by enhancer-driven CNS neuronal markers. (*A–H′*) Expression of four CNS markers in the brains of third instar larvae. In the composite images, the labeled neurons are shown in green and the NC82 counter staining is shown in magenta. (*I–L′′*) Multilabeling of two groups of neurons in adult brains using the GEEM (Gene Expression with an independent Enhancer-driven cellular Marker) technique. The enhancer-driven CD4-tdTom markers (magenta in merged images) label specific neuronal populations and tyraminergic/octopaminergic neurons are labeled by *tyrosine decarboxylase 2* (*TDC2*)-*Gal4 UAS-CD4-tdGFP* (green in merged images). *R9D11-CD4-tdTom* labels a group of neurons targeting the fan-shaped body (Fig. 3 *B–B′′*) and another group occupying suboesophageal ganglion (SOG) (*I*). *R9B07-CD4-tdTom* labels several neurons sending extensive processes to SOG (*K*). The processes of these neurons are shown in higher magnification together with those of TDC2 neurons (*J–J′′* and *L–L′′*; boxed regions in *I* and *K*).

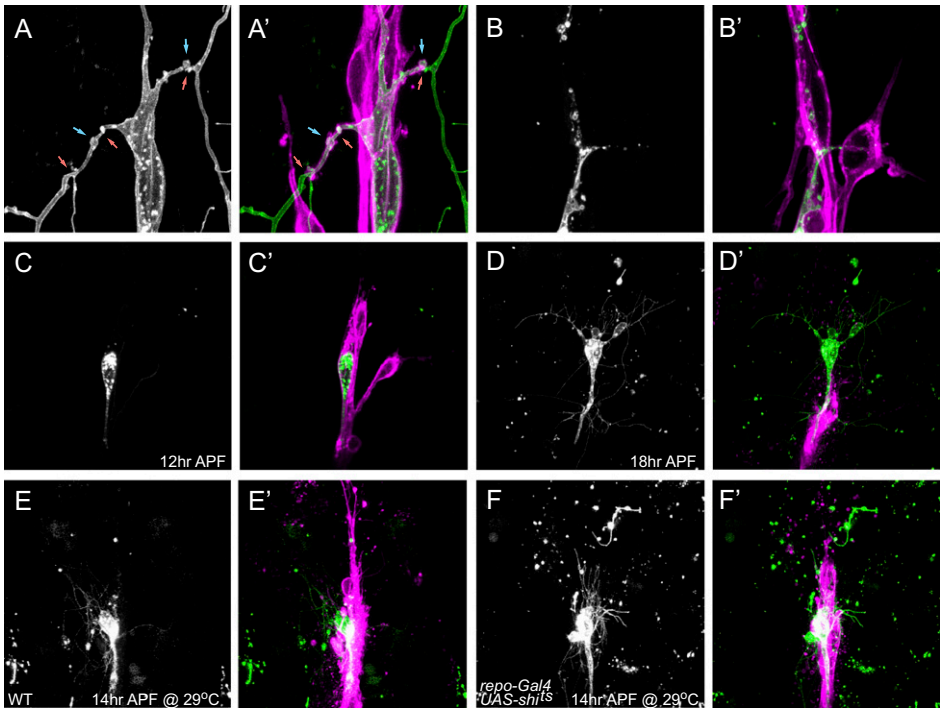


**Fig. S4.** Glial wrapping of C4da neuron ddaC in pupae. (*A* and *A′*) A ddaC neuron imaged at the yellow pupa stage, showing that the constriction (red arrows) and swelling (blue arrows) of proximal dendrites has already started. (*B* and *B′*) A ddaC neuron imaged after severing of proximal dendrites, showing the degradation of wrapped dendrite segments within the glial wrap. (*C* and *C′*) A ddaC neuron imaged at 12 h APF showing the completion of dendrite severing and degradation of wrapped dendrite segments. (*D* and *D′*) A ddaC neuron imaged at 18 h APF showing the disintegration of the glia membrane previously wrapping the ddaC soma and the regrowth of ddaC dendrites. (*E–F′*) ddaC neurons at 14 h APF in a control animal (*E* and *E′*) and an animal expressing $Shi^{ts}$ in glia, both of which were incubated at 29 °C from 3 to 14 h APF. In all panels, the neurons are labeled by *ppk-CD4-tdGFP* (green in merged images) and the glia are labeled by *repo-Gal4 UAS-CD4-tdTom* (magenta in merged images).

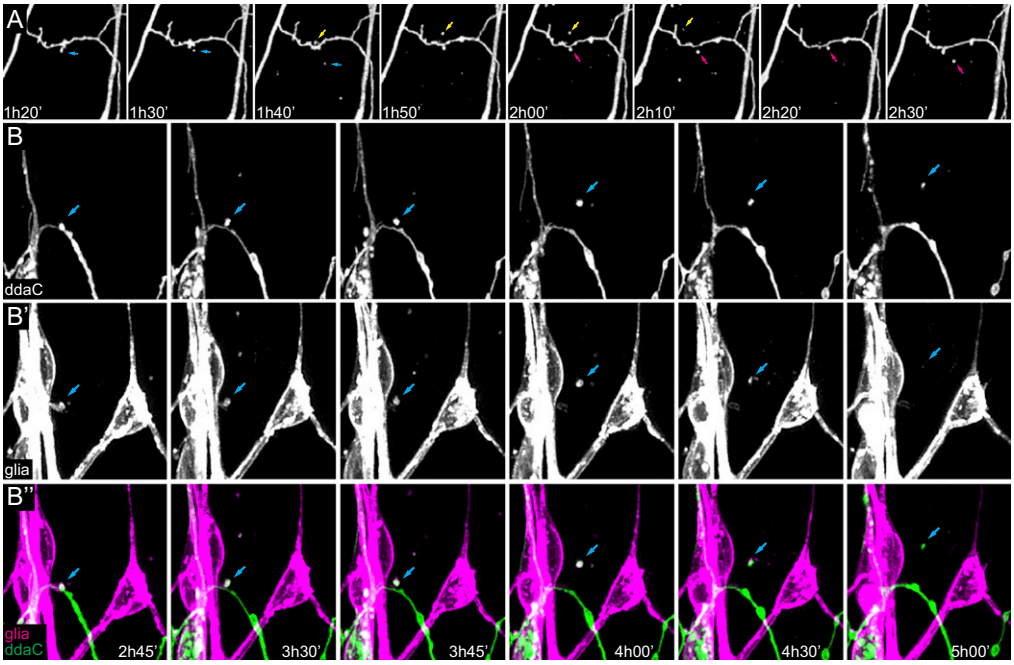


**Fig. S5.** Shedosome formation. (*A*) Time-lapse images showing the detachment of three shedosomes from a dendrite segment in sequence. The first, second, and third shedosomes are indicated by blue, yellow, and magenta arrows, respectively. (*B–B″*) Time-lapse images showing the generation of a shedosome comprised of both dendrite and glial membrane. The glial membrane appears to be degraded before dendrite membrane. In all images, the indicated time are after puparium formation.

**Table S1. PCR fragments used for plasmid construction**

| Fragment | Forward primer | Reverse primer | Template | Purpose |
|---|---|---|---|---|
| CD8-GFP variants in pAPIC | | | | |
| *ppk* enhancer | aataGCGGCCGCacattcaagagttggcaacagg | aattGCTAGCTAAGCtgcgccacacatg | pCaSpeR-ppk-EGFP | pAPIC-PHCH |
| *ppk* enhancer-core promoter-5′UTR | aataGCGGCCGCacattcaagagttggcaacagg | aattCTCGAGGTCCAAAGAGCAGGACTCGTGG | $w^-$ genomic DNA | pAPIC-PCH |
| *hsp70* core promoter-5′UTR | aattGCTAGCgagcgccggagtataaatagag | aattCTCGAGtattcagagttctctccttgtattc | pUAST | pAPIC-PHCH |
| CD8-GFP | tataCTCGAGagaaaACCGGTACGCGTC AAAATGGCCTCACCG | atttTTAATTAAtAGGCCTTATTTGTATAGTTC ATCCATGCCATG | *UAS-CD8-GFP* genomic DNA | pAPIC-PHCH |
| *His2Av* 3′UTR-polyA | aatcTTAATTAACTAAGCCAGTCGGCAA TCGG | atagACTAGTtacgcattttgaaaaacgtcaggtc | $w^-$ genomic DNA | pAPIC-PHCH |
| $\alpha$-*Tub1* 3′UTR-polyA | atttTTAATTAAGCTGAGGAGTACTAAG CGTC | atatACTAGTctcgtagactcgtagttaaattcgg | $w^-$ genomic DNA | pAPIC-PHCT |
| SV40 early 3′UTR-polyA | atttTTAATTAActttgtgaaggaaccttacttctg | atagACTAGTccgatccagacatgataagatac | pUAST | pAPIC-PHCS |
| Synthetic intron | aattGTCGACcagtgactctcttaaggtagcc | aattCTCGAGgagctgtaattgaactgggagtg | pCI-neo (Promega) | pAPIC-PHsICH |
| *hsp70* core promoter-5′UTR-*z* second intron | aattGCTAGCgagcgccggagtataaatagag | aattCTCGAGtcttGGctaaacgaaaaggaagaatttag actttgaaggggatctttaagaagggtgtacaatctcac Cggcagatttcagtagttgcag | pUAST | pAPIC-PHzICH |
| *eve* core promoter-5′UTR | aataGCTAGCAGCGCAGCGGTATAAA AGGG | gagtcactgCGTCTTGTGATTCAAAGTTGGC | $w^-$ genomic DNA | pAPIC-PEsICH |
| Synthetic intron | CACAAGACGcagtgactctcttaaggtagcc | aattGTCGACgagctgtaattgaactgggagtg | pCI-neo | pAPIC-PEsICH |
| CD4-GFP, CD4-tdGFP, and CD4-tdTomin pAPIC | | | | |
| sSP | ttttACGCGTgaattccaaagATGCCACCTTC | GGAACGAGCCTCCACCTCCACTTCCGCCGCCA CCGCTAGCAGTGACTTCTCCAG | ace-4p-CD4-2-spGFP (1) | pAPIC-ppk-CD4-GFP |
| CD4 transmembrane domain | GAGGTGGAGGCTCGTTCCAGAAGGCCT CCAGCATAGTC | ttttggatccGCCTCCGCTTCCGCCGCGCCTTCGG TGCCGGCACCTGACAC | ace-4p-CD4-2-spGFP | pAPIC-ppk-CD4-GFP |
| EGFP (first half of tdGFP) | atttggatcccgtagtcgtgcccaggcttccGT GAGCAAGGGCGAGGAGCTG | aaatTCCGGAGCTGCCGCTGCCGGTGCTGCCGG TGCCATGCCCCATGCCGAGAGTGATCCCG | pEGFP-N1 (Clontech) | pAPIC-sSP-CD4-tdGFP |
| GFP (second half of tdGFP) | aaatTCCGGAACCGCCTCCTCCGAGGAC AACAACATGGCCAGTAAAGGAGAAG AACTTTTCACTGG | aattTCTAGATTAgctgtttgcgttctcGTAgAGTTCA TCCATGCCATGTGTAATC | pAPIC-PHCH | pAPIC-sSP-CD4-tdGFP |
| tdGFP-ER(Kir2.1) | ggatcccgtagtcgtgcccaggcttcc | aattTCTAGATTAgagggcaacttcattttcatagcaaaa gctgtttgcgttctcGTAgAG | pAPIC-sSP-CD4-tdGFP | pAPIC-sSP-CD4-tdGFP-ER(Kir2.1) |
| *Akh* signal peptide | aattccaaaATGAATCCCAAGAGCGAAGTC CTCATTGCAGCCGTGCTgTTCATGCTGCT GGCCTGCGTCCAGTGTCAAG | CTAGCTTGACACTGGACGCAGGCCAGCAGCAT GAAcAGCACGGCTGCAATGAGGACTTCGCTC TTGGGATTCATtttgg | NA | pAPIC-Akh-CD4-tdGFP-ER(Kir2.1) |
| tdTom | attaggatccATGGTGAGCAAGGGCGAGGAG | aattTCTAGATTAgagggcaacttcattttcatagcaaaa gctgtttgcgttctcCTTGTACAGCTCGTCCATGCC | pRSET-B-dTomato | pAPIC-CD4-tdTom |
| pHemmarG-ppk and pHemmarR-ppk | | | | |
| *ppk* enhancer | ggggACAAGTTTGTACAAAAAAGCAGGCT acattcaagagttggcaacagg | ggggACCACTTTGTACAAGAAAGC TGGGTTAAGCtgcgccacacatg | pCaSpeR-ppk-EGFP | pENTR-ppk |

1. Feinberg EH, et al. (2008) GFP Reconstitution Across Synaptic Partners (GRASP) defines cell contacts and synapses in living nervous systems. *Neuron* 57:353–363.

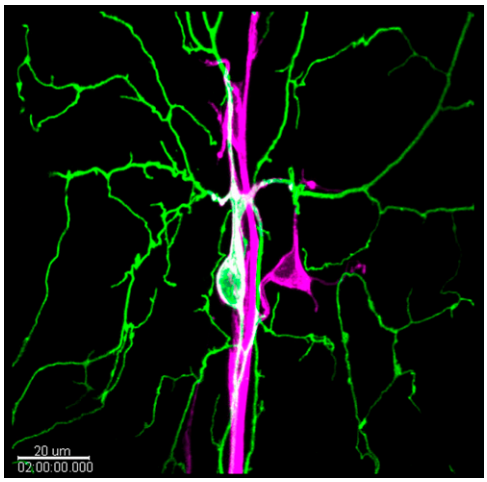


**Movie S1.** Severing of proximal dendrites of ddaC neurons in dendrite pruning. Time-lapse movie of a *ppk-CD4-tdGFP; repo-Gal4 UAS-CD4-tdTom* prepupa between 2 and 9 h APF. The ddaC neuron is in green and the glial membranes are in magenta. Selected frames are shown in Fig. 5 *E* and *E′*.

Movie S1